NYO - 3862

A FAST NEUTRON SPECTROMETER

G. E. OWEN and P. R. CHAGNON

The Johns Hopkins University

BALTIMORE, MARYLAND

AEC Contract No. AT(30-1)–1251

OCTOBER, 1953

UNCLASSIFIED

NYO - 3862

A FAST NEUTRON SPECTROMETER

G.E. Owen and P.R. Chagnon

The Johns Hopkins University

Baltimore, Maryland

AEC Contract No. AT(30-1)-1251

October, 1953

UNCLASSIFIED

CONTENTS

INTRODUCTION

The detection of neutrons is in general more difficult than the detection of charged particles. In particular, the measurement of neutron energies is time-consuming and cannot be performed with the accuracy that can be obtained in the determination of the energies of charged particles. In the past the two major methods used in the determination of neutron energies have been the proportional counter[1] and the nuclear emulsion technique[2]. Although both of these methods have been responsible for the wide knowledge of neutron spectra that is at present available, it is still difficult to obtain both efficiency and resolution from a single method.

The scintillation counter which employs a hydrogenous scintillator provides another method whereby neutrons can be studied in terms of the proton recoil distribution produced within the scintillator. For neutron energies less than 20 Mev, the recoil protons have an energy distribution which is ideally a step function. Figure 1[3] shows a typical pulse height distribution which arises when a trans-stilbene scintillator is irradiated by 2.5 Mev neutrons. Distortions arising from statistical fluctuations in the scintillator and photomultiplier, non-linearity, energy spread of the incident neutron, etc.[3] cause the observed deviation from the ideal step function. It is evident that when two or more neutron energy groups are present, the continuous proton recoil spectrum becomes quite difficult to analyze.

In the case of gamma-rays, Hofstadter[4] has developed a two crystal coincidence technique to convert a continuous Compton electron recoil spectrum to a line spectrum. A secondary scintillator is utilized in coincidence with the primary scintillator to select Compton recoil gamma-rays at a fixed angle. Pulses due to recoiling electrons in the primary counter are

1. D.H. Frisch, Phys.Rev. 70, 589 (1946). Coon and Nobles, Rev.Sci. Inst. 18, 44 (1947); Nereson and Darden, Phys.Rev. 89, 775 (1953).
2. Taylor, Proc.Roy.Soc. 150, 382 (1935). Blau, Jour.Phys. et Rad. 5, 61 (1934); H.T. Richards, Phys.Rev. 59, 796 (1941); C.F. Powell, Proc. Roy.Soc. 181, 344 (1943); R.A. Peck, Phys.Rev. 73, 947 (1948).
3. Segel, Swartz, and Owen: Rev.Sci.Inst., to be published.
4. Hofstadter and McIntyre, Phys.Rev. 78, 619 (1950).

Fig. 1. The pulse height distribution produced in a trans-stilbene scintillator by D-D neutrons

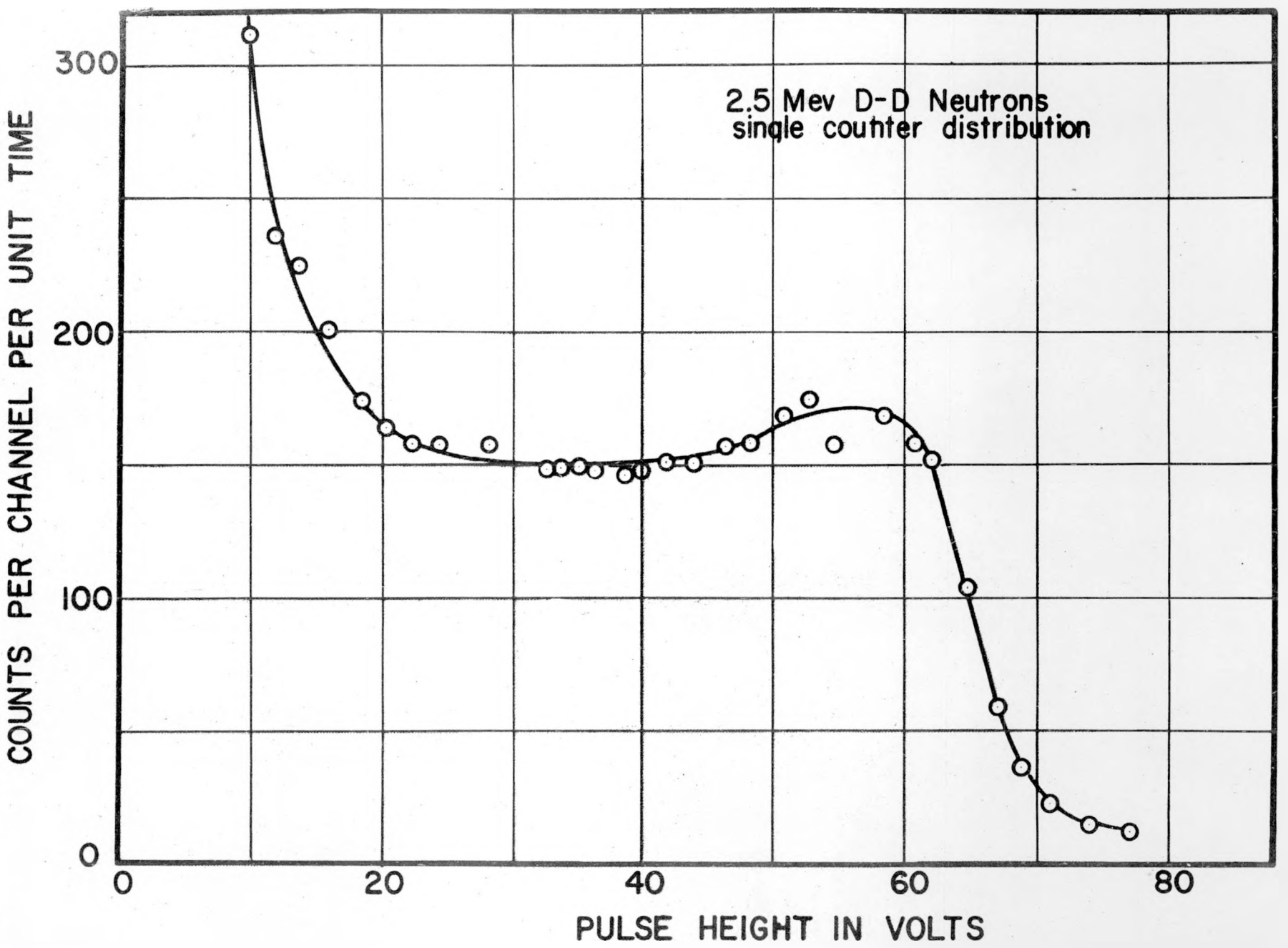
2.5 Mev D-D Neutrons
single counter distribution
COUNTS PER CHANNEL PER UNIT TIME
PULSE HEIGHT IN VOLTS
0
100
200
300
0
20
40
60
80

Fig. 2. Drawing of the spectrometer frame. The paraffin shield is not shown in this diagram.

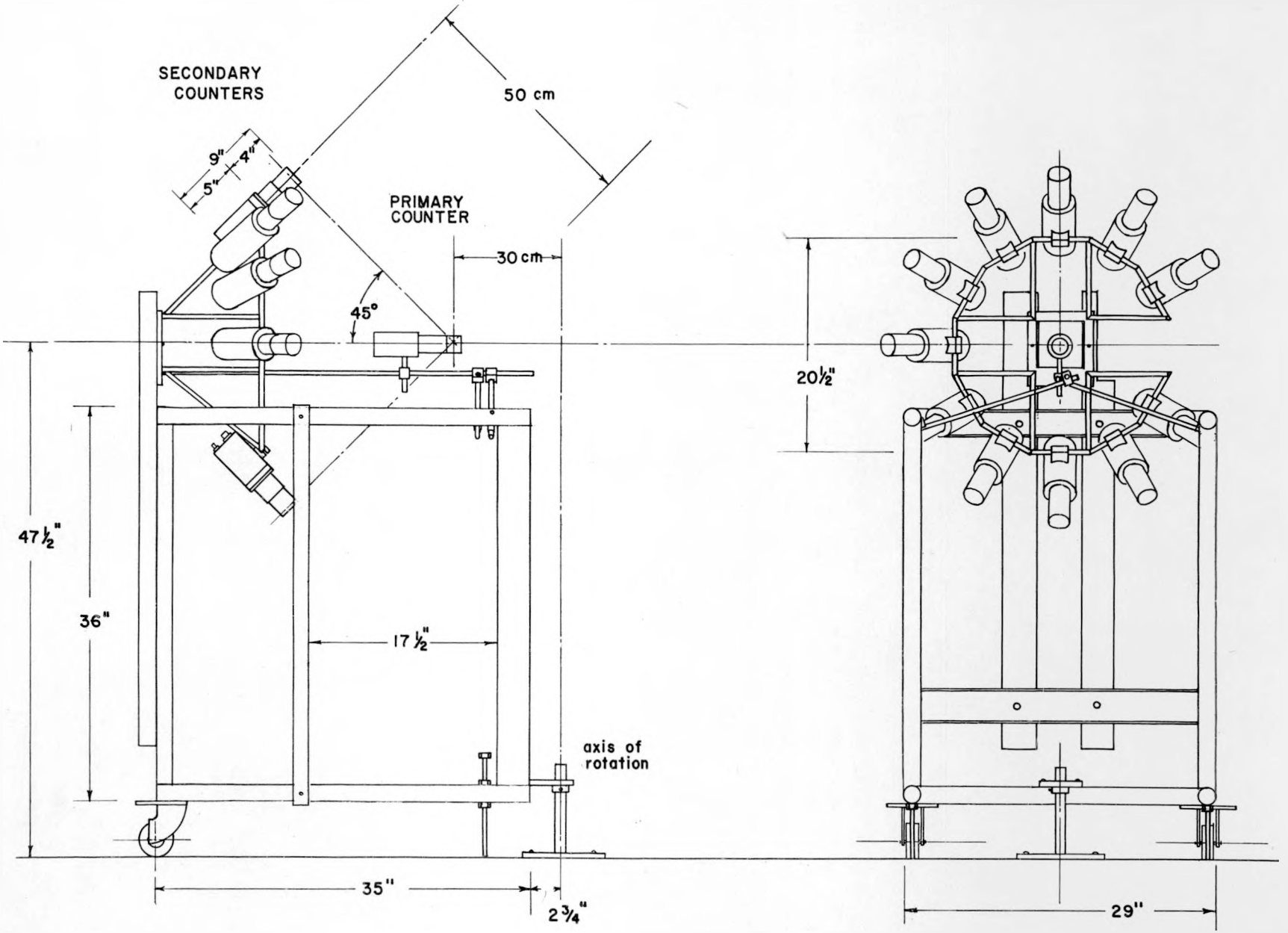

FAST NEUTRON SPECTROMETER

DETAIL OF THE FRAME

gated by coincidence pulses from both counters. Thus the only pulses recorded are those corresponding to scattering of the photon through a given angle, and therefore due to electrons of a unique energy if the incident photons are monochromatic.

A similar method can be used for the detection of neutrons scattered by protons. In the case of neutrons, advantage can be taken of the long time of flight of the scattered neutron which allows discrimination between neutrons and gamma-rays. A detection technique involving only the time of flight of the neutrons is being developed[5]. Calculations[6a] pertaining to, and tests[7, 8, 6b] of such an instrument have been reported. An improved instrument having a relatively high efficiency will be discussed in the following paragraphs.

Design and Construction

The first instrument[6b] tested by the authors employed a secondary ring of liquid scintillators placed on the circumference of a circle having a radius of one meter. Because of self absorption of light in the liquid counters, the efficiency of the spectrometer was low. At the same time the large volume of scintillating material produced a high ratio of background counts to true counts.

The present spectrometer utilizes as a secondary ten trans-stilbene cylinders placed upon the circumference of a circle of 35 cm. radius. (See Figures 2 and 3.) These scintillators have a high efficiency coupled with a low background-to-signal ratio.

In Fig. 4 the basic target and two-crystal geometry are shown. T is the source of neutrons, P is the primary or scattering counter, and S is one of the secondary counters. θ is the angle between center lines,

---

5. Jennings and Griffith, Phys.Rev. 91, 440 (1953).
6a. Neiler, Owen, and Allen, Phys.Rev. 83, 242 (1951).
7. Draper and McDaniel, Phys.Rev. 87, 185 (1952).
8. Beghian, Allen, Calvert, and Halban, Phys.Rev. 86, 1044 (1952).
6b. Chagnon, Madansky, and Owen, Rev.Sci.Inst. 24, 656 (1953).

Fig. 4. The target and scintillator geometry

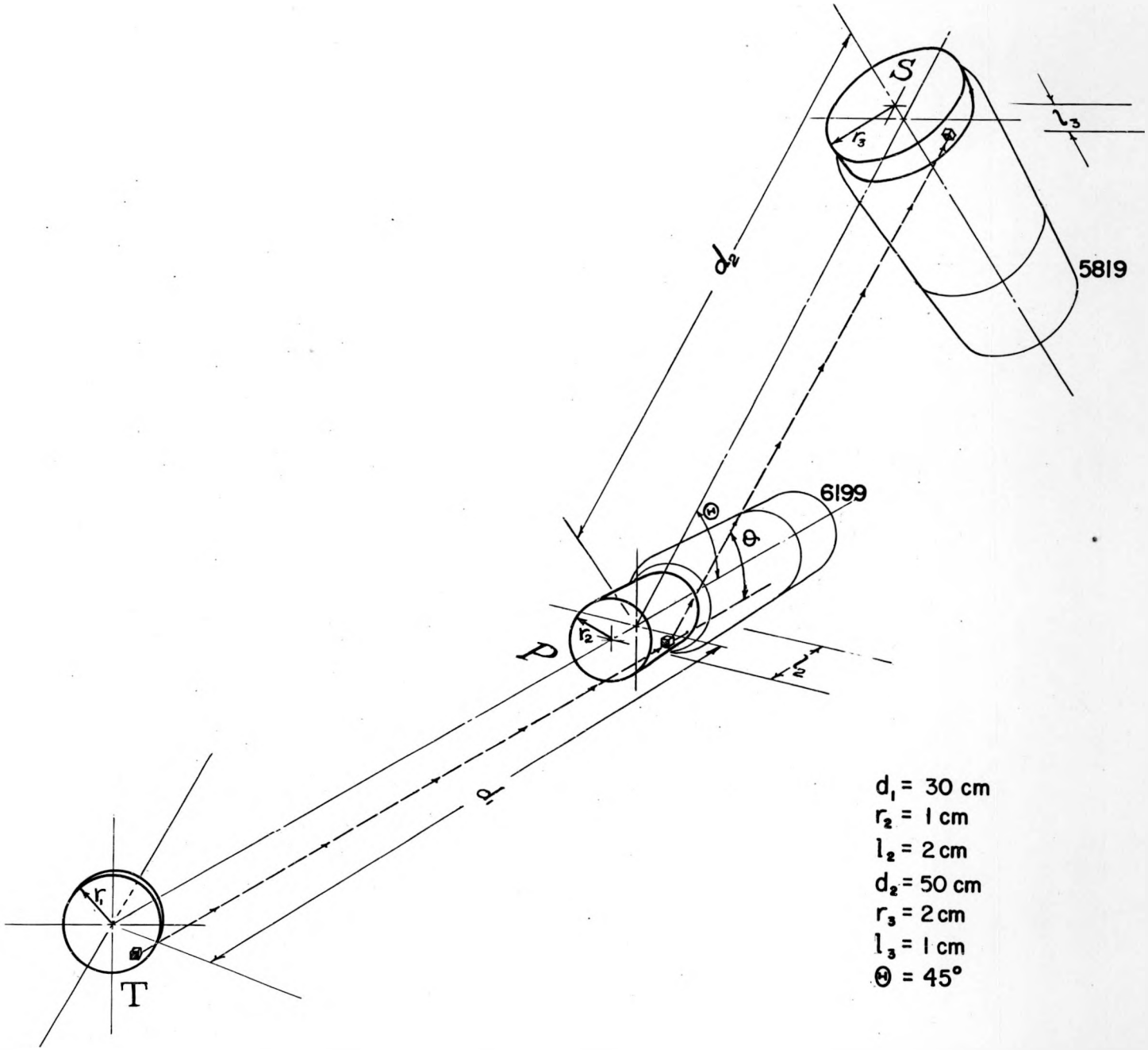

d_1 = 30 cm
r_2 = 1 cm
l_2 = 2 cm
d_2 = 50 cm
r_3 = 2 cm
l_3 = 1 cm
Θ = 45°

and Θ is an arbitrary scattering angle. When a neutron of energy E_n is scattered from a proton in P through an angle Θ, the scattered neutron has an energy $E_n \cos^2\Theta$ and the recoil proton has an energy $E_n \sin^2\Theta$, resulting in a pulse height H^o_p. Thus H^o_p is a direct measure of the incident neutron energy.

A detailed discussion of the resolution and efficiency has been reported[6] previously. Therefore only the result as applied to the instrument under discussion will be presented. In the study of neutrons of energy E_n a distribution of pulse heights $f(H_p)$ is observed. The factors contributing to the width of this distribution are:

1. Imperfect definition of the scattering angle. The standard deviation corresponding to this distortion is σ_Θ

2. Crystal and phototube statistics, with a corresponding standard deviation σ_c

3. Short term fluctuations in the amplification giving a standard deviation σ_a

4. Finite width of the channels in the multichannel discriminator. This standard deviation is σ_d

Since $f(H_p)$ is the convolution of the several distribution densities describing these effects, it can be approximated quite well by a Gaussian form:

$$f(H_p) \approx \frac{1}{\sigma\sqrt{2\pi}} e^{-\frac{(H_p - H_p^o)^2}{2\sigma^2}} \qquad (1)$$

The resolution of the instrument is given by

$$R = \frac{2\sigma}{H_p^o} = \frac{2}{H_p^o}\left\{\sigma_\Theta^2 + \sigma_c^2 + \sigma_a^2 + \sigma_d^2\right\}^{1/2} \qquad (2)$$

Using the geometry presented in Fig. 4,

$$\sigma_\theta = (12)^{-1/2}\left[\frac{2H_p^\circ}{\tan\Theta}\right]\left\{6\left(\frac{r_1}{d_1}\right)^2 + 4\left(\frac{r_2}{d_1}\right)^2\left(1+\frac{l_2}{2d_1}\right)^2 + \left(\frac{l_2}{d_2}\right)^2\left(\sin\Theta + 3\frac{r_2}{l_2}\cos\Theta\right)^2 + \left(\frac{l_3}{d_2}\right)^2\left(1+\frac{r_3^2}{2d_2 l_3}\csc\Theta\right)^2\right\}^{1/2} \quad (3)$$

$$\sigma_d = (12)^{-1/2}(\Delta H)$$

σ_c and σ_a can be measured for a specific arrangement. In the case under consideration,

$$\sigma_\theta \cong 0.062\ H_p^\circ$$

$$\sigma_c \cong 0.09\ H_p^\circ\ (2\,\text{Mev}/E_n)^{1/2}$$

$$\sigma_a \cong 0.02\ H_p^\circ$$

and

$$\sigma_d \cong 0.14\ H_p^\circ$$

These values allow a resolution of 12 percent. However, in all of the neutron data which have been taken, thick targets have been employed. Because of this, line shapes suffer a further spread.

If the total number of neutrons per unit time which enter P is N_o, and if the coincidence rate is C, the efficiency can be written as

$$\epsilon = \frac{C}{N_o} = \frac{2r_3 l_3}{\pi d_2^2}\left(1-e^{-K l_2 \sigma(E_n)}\right)\left(1-e^{-\frac{K\pi r_3 \sigma(E_n\cos^2\Theta)}{2}}\right)\cos\Theta\left\{\frac{E_n\cos^2\Theta - E_D}{E_n\cos^2\Theta}\right\} \quad (5)$$

The values and explanation of d_2, l_2, r_3 and l_3 are given in Fig. 4. K is the number of hydrogen atoms per centimeter per barn in the trans-stilbene scintillator. $\sigma(E_i)$ is the n,p cross section in barns for an energy E_i, and E_D is the discrimination level of the coincidence circuit for pulses from the secondary counters. The value of E_D in the present experiments is approximately 0.2 Mev.

A plot of equation (5) is shown in Fig. 5. It has been pointed out[9]

---

9. J.O. Elliot, private communication.

that multiple scattering in the primary crystal P will reduce the overall efficiency by a measurable amount. A correction factor exp. $\left(-K r_2 \sqrt{2}\, \sigma(E_n/2)\right)$ has been applied as a first approximation, and the result is also shown in Fig. 5.

The scattering angle θ is 45°. Angles near 45° allow good efficiency and good resolution. The geometrical factor σ_θ is small at large angles; however, the efficiency becomes quite low at large angles, mainly because the counting rate in the secondary counters drops as a constant minus $1/\cos^2\theta$. The range of practicable angles lies between 30° and 60°. A setting of 45° seems to be satisfactory.

The construction details of the neutron spectrometer are shown in Fig. 2 and Fig. 3. All scintillators are trans-stilbene. Each crystal is mounted inside of a cylindrical metallic holder which is cemented to the phototube in the case of the primary counter (RCA 6199) and to a lucite light piper in the case of the secondary counters (RCA 5819). A thin layer of silicone grease is deposited between the crystal and the phototube or light piper. The outer surfaces of the crystals are packed with a magnesium oxide layer. A large conical paraffin shield is placed between the secondary counters and the target. This shield is shown in Fig. 3.

A block diagram of the associated electronic circuits is shown in Fig. 6. Pulses from the ten secondary photomultipliers are fed into a fast mixer[10]. The output of the fast mixer is amplified by a fast cascade amplifier before passing to the coincidence circuit. Two pulses are obtained from the primary counter: one from the anode and one from the last dynode. The dynode pulse is amplified by a similar fast amplifier and passes to the coincidence circuit. The output of the fast amplifiers provides pulses of a constant amplitude over a wide interval of the secondary recoil proton spectrum. The pulses are then clipped by 1 meter shorted stubs of Transradio type C3 coaxial cable.

Two types of coincidence circuits have been employed, one using vacuum tubes and the other germanium diodes. Both utilize the nonlinear load introduced by Garwin[11]. The diode circuit results in a slightly more rectangular shaped delay discriminator characteristic. The rather short resolving time of this circuit requires the introduction of sufficient delay to compensate for the different lengths of connecting cables and for the neutron time of flight. On the other hand, the resolving time is large enough to allow a range of neutron energies to be selected.

---

10. P. Chagnon, L. Zernow, and L. Madansky, Rev.Sci.Inst. 24, 326 (1953)
11. R.L. Garwin, Rev.Sci.Inst. 21, 569 (1950)

Fig. 5. The efficiency of the fast neutron spectrometer as calculated from equation 5, using the parameters given in Fig. 4

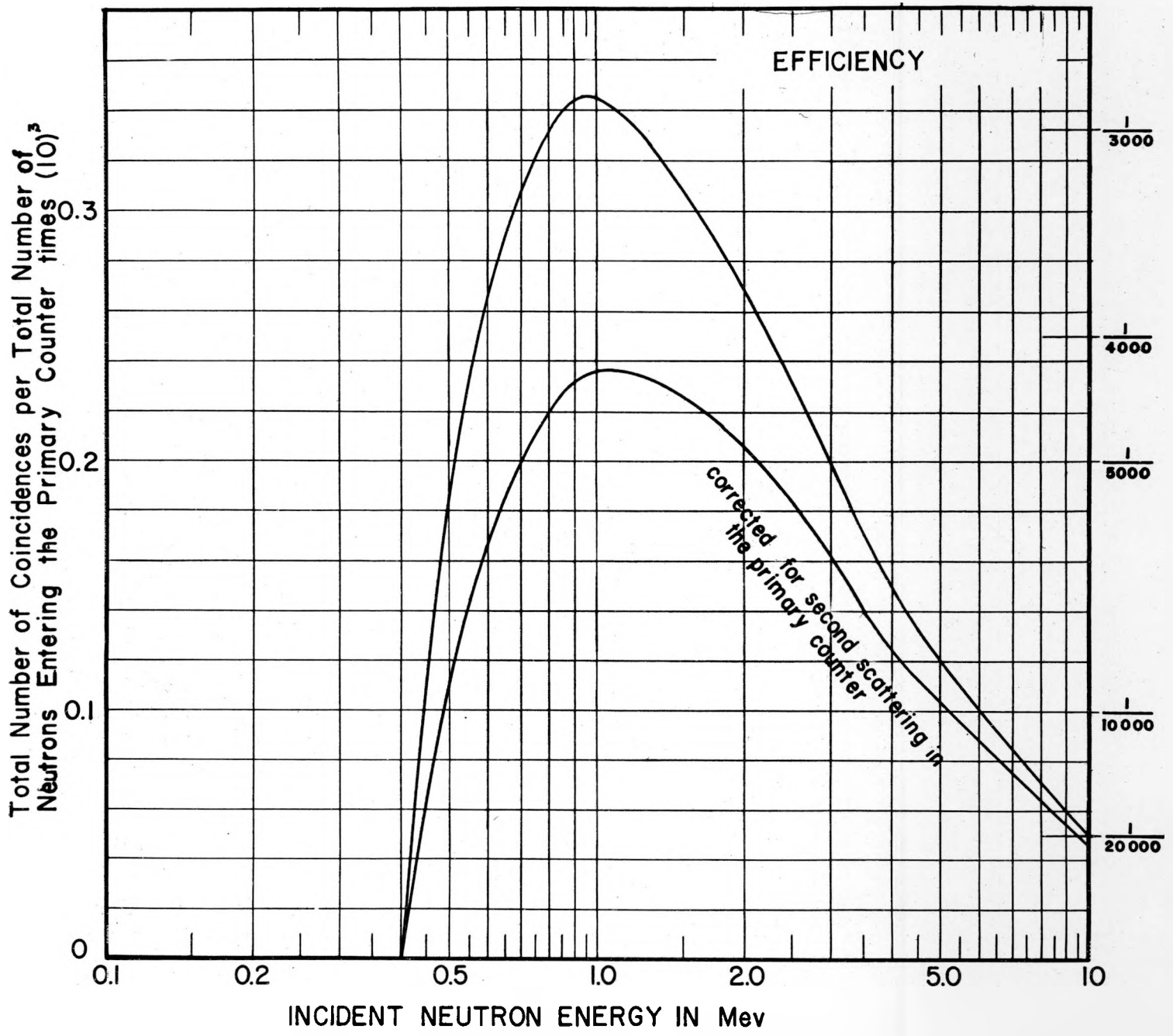
EFFICIENCY
1/3000
1/4000
1/5000
1/10000
1/20000
corrected for second scattering in the primary counter
Total Number of Coincidences per Total Number of Neutrons Entering the Primary Counter times (10)³
0
0.1
0.2
0.3
0.1
0.2
0.5
1.0
2.0
5.0
10
INCIDENT NEUTRON ENERGY IN Mev

Fig. 6. Block diagram of the electronic circuits

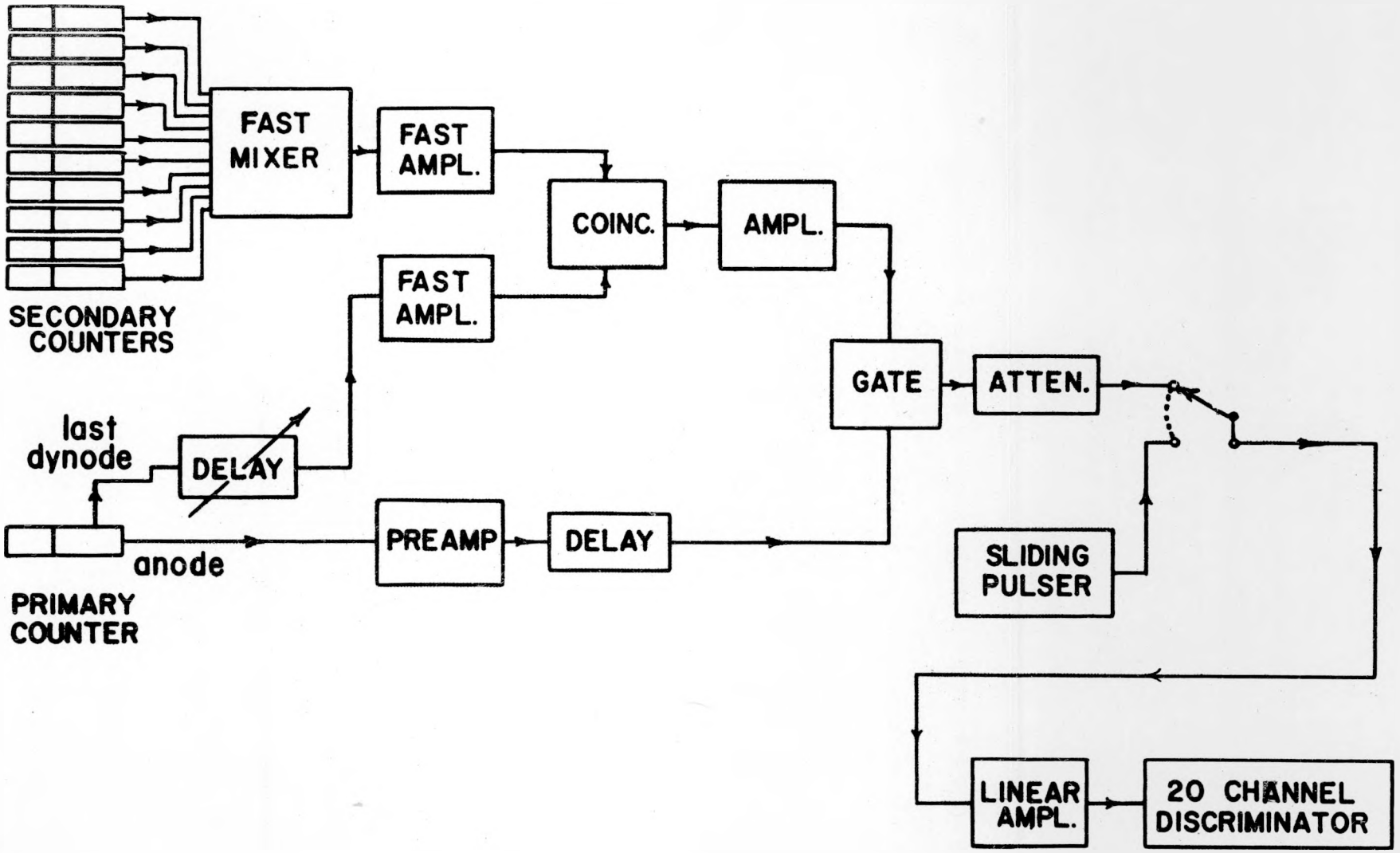

CIRCUIT BLOCK DIAGRAM
of the FAST NEUTRON SPECTROMETER

The output pulse from the coincidence circuit triggers a low level gate circuit[12] which permits the pulse from the anode of the primary counter to pass undistorted to the linear amplifier. The output of the linear amplifier is then analyzed by a twenty channel discriminator.

Performance

The fast coincidence spectrometer will record the spectra of gamma-rays or of neutrons depending upon the amount of delay interposed between the primary signal and the secondary signal. At present the instrument is being used for spectral analysis and angular distributions both of gamma-rays and of neutrons arising from (d, n) reactions in the light elements.

In the following discussion all of the neutron spectra were obtained from reactions involving thick targets. Therefore the line width obtained in these experiments does not illustrate the limit of the resolution of the instrument; in the case of the D-D neutrons, the spread in neutron energy introduced by the thick target accounts for more than 50 percent of the total line width at some angles.

The time of flight difference between the D-D neutrons and Co^{60} gamma-rays is illustrated in Fig. 7. The delay discriminator characteristic is shown for the two types of particles in terms of the delay between the primary and secondary pulses. The zero of Fig. 7 actually represents a delay of 1.7 millimicroseconds, which is the time of flight for gamma-rays between the primary and secondary counters.

In Fig. 8 the pulse height spectrum of the two Co^{60} gamma-rays is shown. This spectrum was obtained by setting the delay to the zero shown in Fig. 7.

Fig. 9 illustrates the pulse height spectrum of the neutrons from the D-D reaction. The deuteron bombarding energy was 0.6 Mev, and the delay had been set at 29 millimicroseconds, which is the time of flight for neutrons of one half the incident energy of 3.22 Mev. The intensity variations shown in Fig. 9 for D-D neutrons emitted at various angles with respect to the beam have not been corrected for either the instrument efficiency as a function of energy or for the variation of efficiency as a function of time of flight when the delay is fixed. It has been pointed out that these line widths

---

12. Paul R. Chagnon, Rev. Sci. Inst., 24 (1953)

Fig. 7. Time of flight spectrum for the gamma-rays of Co^{60} and neutrons from the D-D reaction. The total coincidence rate is plotted as a function of the time delay between the primary and secondary counters.

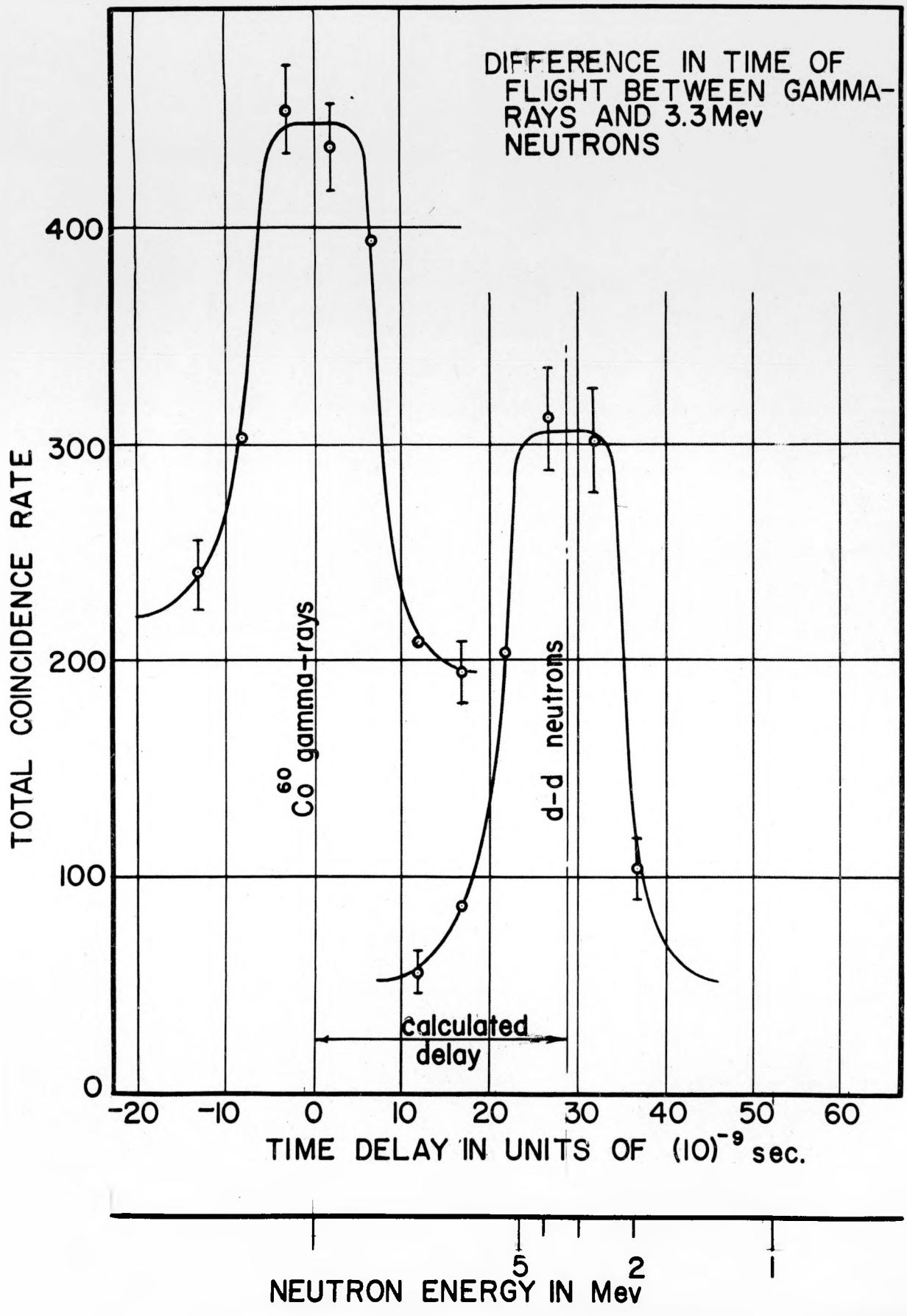
DIFFERENCE IN TIME OF FLIGHT BETWEEN GAMMA-RAYS AND 3.3 Mev NEUTRONS
TOTAL COINCIDENCE RATE
400
300
200
100
0
Co^{60} gamma-rays
d-d neutrons
calculated delay
-20
-10
0
10
20
30
40
50
60
TIME DELAY IN UNITS OF $(10)^{-9}$ sec.
5
2
1
NEUTRON ENERGY IN Mev

Fig. 8. The gamma-ray spectrum of Co^{60}. The peaks correspond to gamma-ray energies of 1.17 and 1.34 Mev.

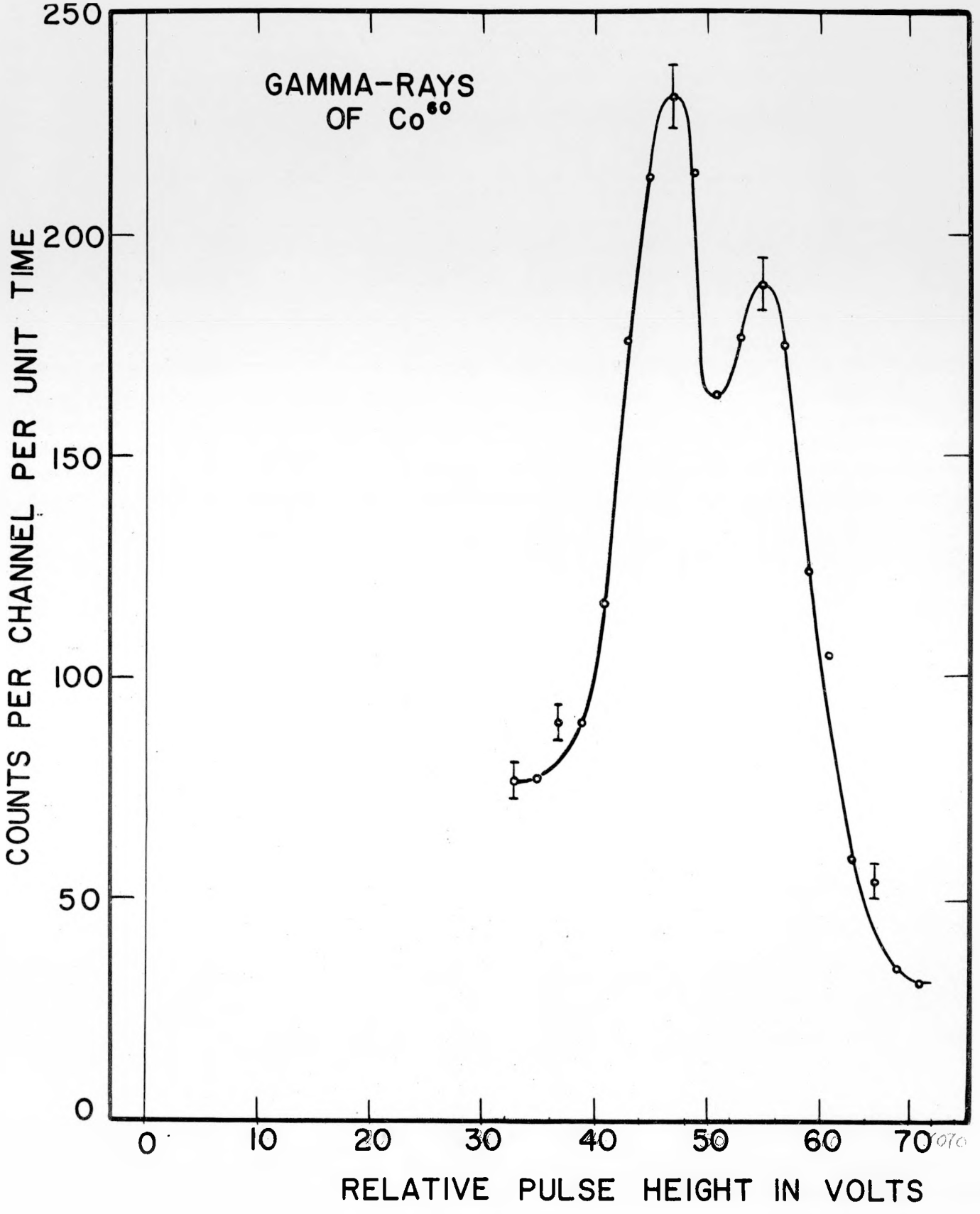
GAMMA-RAYS
OF Co60
250
200
150
100
50
0
COUNTS PER CHANNEL PER UNIT TIME
0
10
20
30
40
50
60
70
RELATIVE PULSE HEIGHT IN VOLTS

Fig. 9. The pulse height spectrum of the neutrons from the D-D reaction. The deuteron bombarding energy was 600 kev.

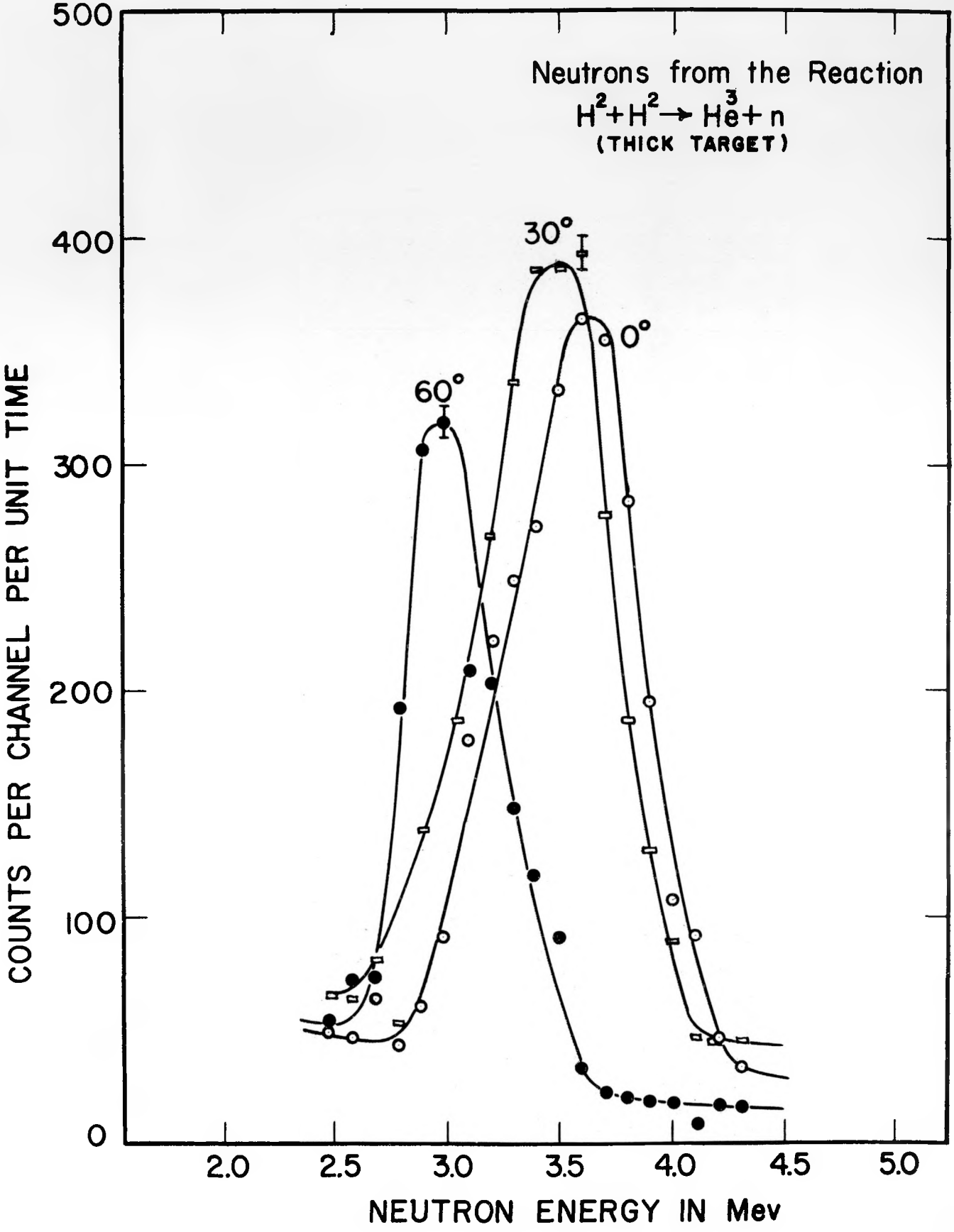
Neutrons from the Reaction
$H^2+H^2 \rightarrow He^3+n$
(THICK TARGET)
30°
0°
60°
COUNTS PER CHANNEL PER UNIT TIME
NEUTRON ENERGY IN Mev
500
400
300
200
100
0
2.0
2.5
3.0
3.5
4.0
4.5
5.0

shown in Fig. 9 do not represent the resolution of the instrument because of the presence of a large amount of thick target distortion.

A study both of the gamma-rays and of the neutrons from the reaction, $Be^9 + H^2$, is being conducted. The time of flight distribution of the products is illustrated by the delay discriminator curve of Fig. 10. It is interesting to note that not only is there discrimination between the neutrons and gamma-rays, but also the variation in intensity of the various neutron energy groups (see below, Fig. 12) shows up in the time of flight spectrum.

By setting the delay at the zero of Fig. 10, the 0.72 Mev gamma-ray and 1.02 Mev gamma-ray produced in the reaction $Be^9(d,n)B^{10*}(\ )B^{10}$ were obtained within the range of a single bias setting of the twenty channel discriminator. The pulse height distribution associated with the 0.72 Mev and 1.02 Mev gamma-rays is shown in Fig. 11.

Previous investigations[13] have shown that several neutron groups result from the reaction $Be^9(d,n)B^{10}$ for bombarding energies in the neighborhood of 1 Mev. The four neutron groups of highest energy have been investigated in a preliminary manner with the coincidence spectrometer. The pulse height spectrum corresponding to these neutron groups is shown in Fig. 12. In this spectrum the background due to accidental coincidences is quite high. Since the time of this experiment, the high background has been reduced by reducing the overall resolving time of the coincidence system.

Conclusions

This method of applying the technique of scintillation spectroscopy to the study of neutrons seems to be very promising. The relatively high efficiency of the instrument made it possible to obtain the neutron data shown in Fig. 12 in a running time of approximately three hours, using a bombarding deuteron current of approximately 1/4 microampere. The short resolving time of the coincidence circuit permits operation of the instrument in the presence of a high intensity of background radiation. It is hoped that this property can be extended sufficiently to permit studies of neutron scattering.

It may be pointed out that only with the scintillation spectrometer can studies be made of selected neutron groups with other particles: for example, the n, γ correlations in several (d, n) reactions.

---

14. Staub and Stephens, Phys.Rev. 55, 135 (1939); C.F. Powell, Proc. Roy.Soc. (London) A 181, 344 (1943); F. Ajzenberg, Phys.Rev. 82, 43 (1951); 88, 298 (1952); Pruitt, Hanna and Swartz, Phys.Rev. 87, 534 (1952)

Fig. 10. The time of flight spectrum for the gamma-rays and neutrons from the reaction $Be^{9} + H^{2}$.

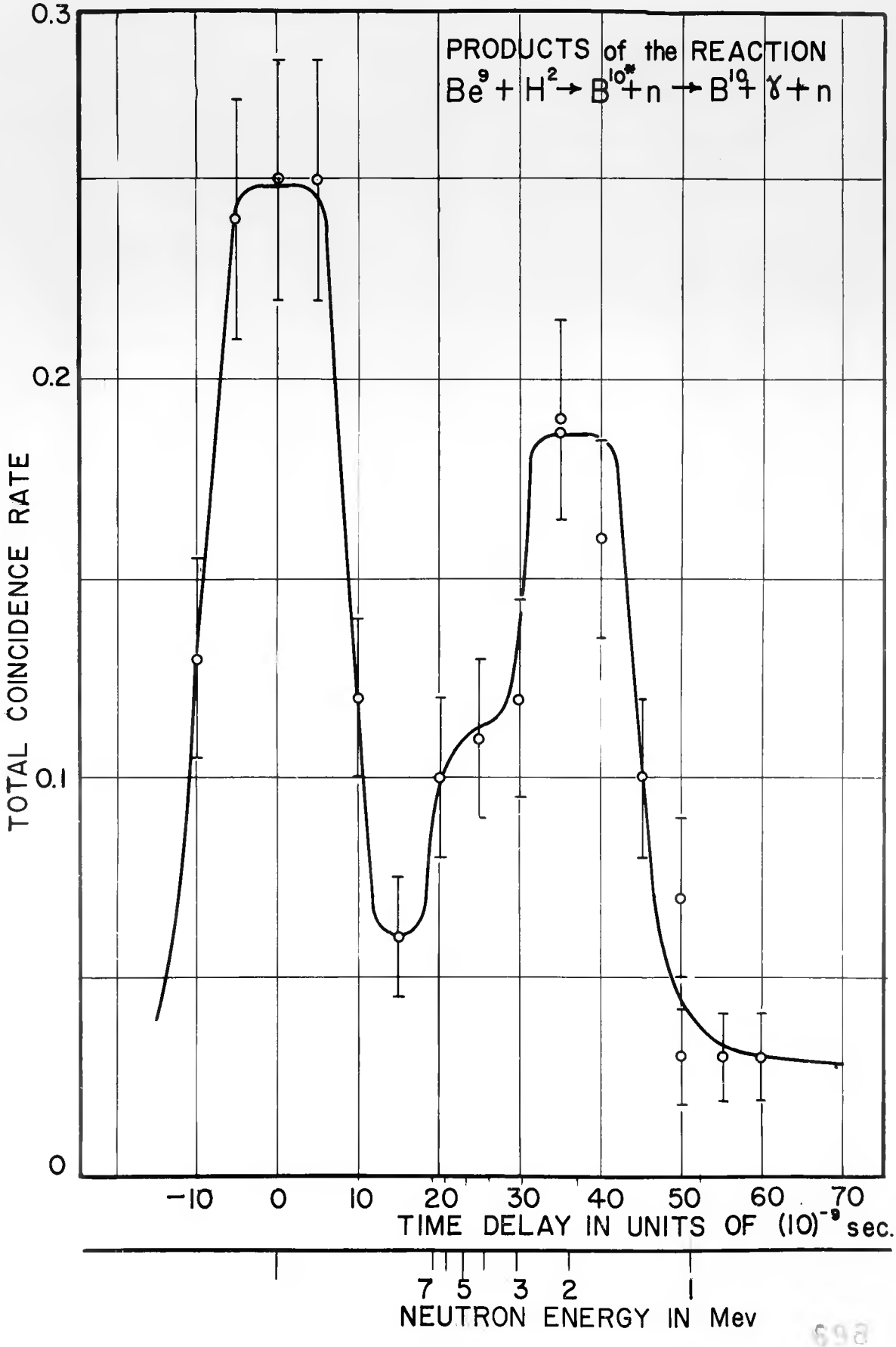
PRODUCTS of the REACTION
$Be^9 + H^2 \rightarrow B^{10*} + n \rightarrow B^{10} + \gamma + n$
TOTAL COINCIDENCE RATE
0.3
0.2
0.1
0
−10
0
10
20
30
40
50
60
70
TIME DELAY IN UNITS OF $(10)^{-9}$ sec.
7
5
3
2
1
NEUTRON ENERGY IN Mev

Fig. 11. The spectrum of the 0.72 Mev and 1.02 Mev gamma-rays from the reaction $Be^9 + H^2$

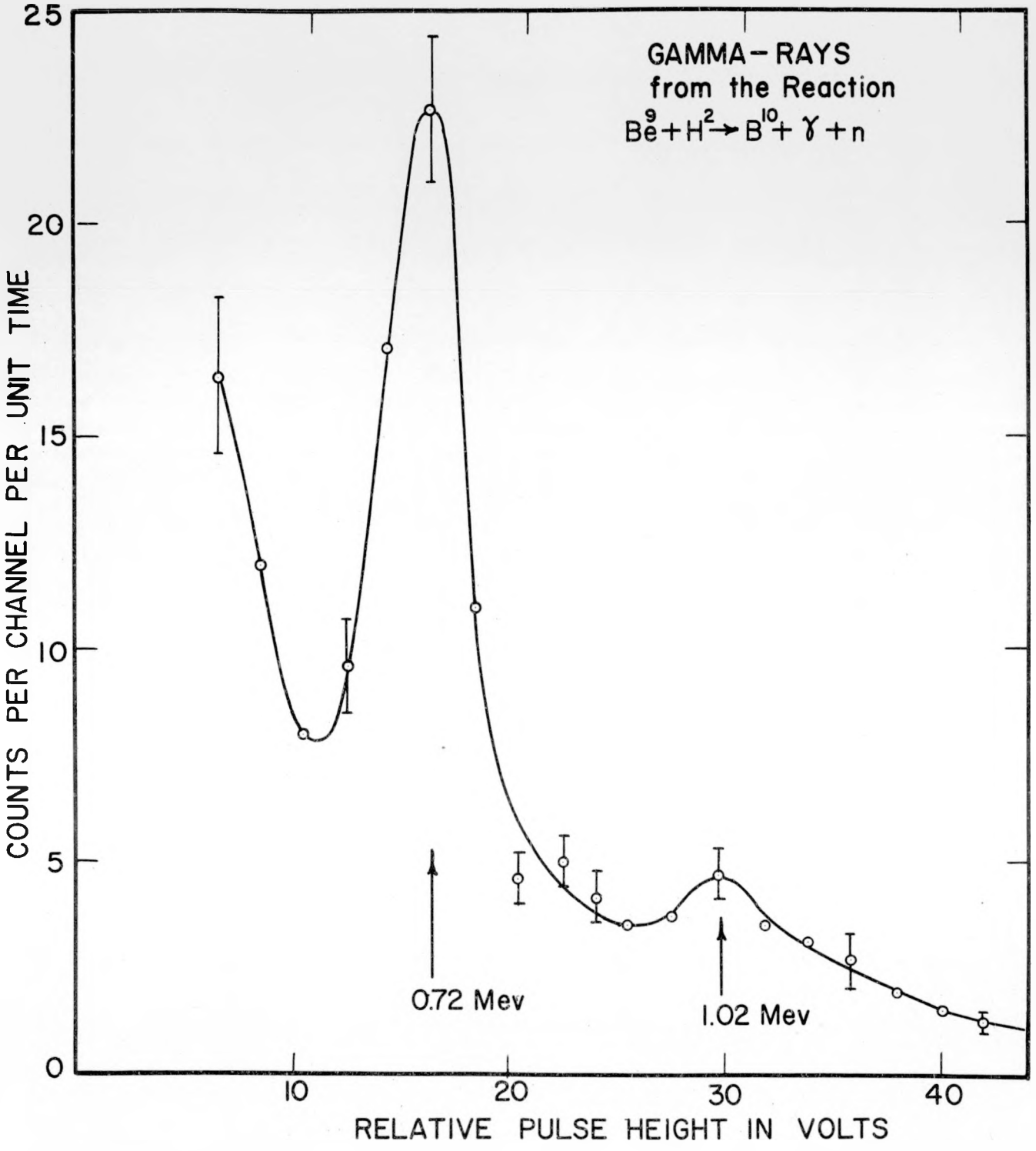
GAMMA-RAYS
from the Reaction
$Be^{9}+H^{2}\rightarrow B^{10}+\gamma+n$
COUNTS PER CHANNEL PER UNIT TIME
RELATIVE PULSE HEIGHT IN VOLTS
0.72 Mev
1.02 Mev
0
5
10
15
20
25
10
20
30
40

Fig. 12. The four neutron groups of highest energy from the reaction

$Be^9 + H^2$

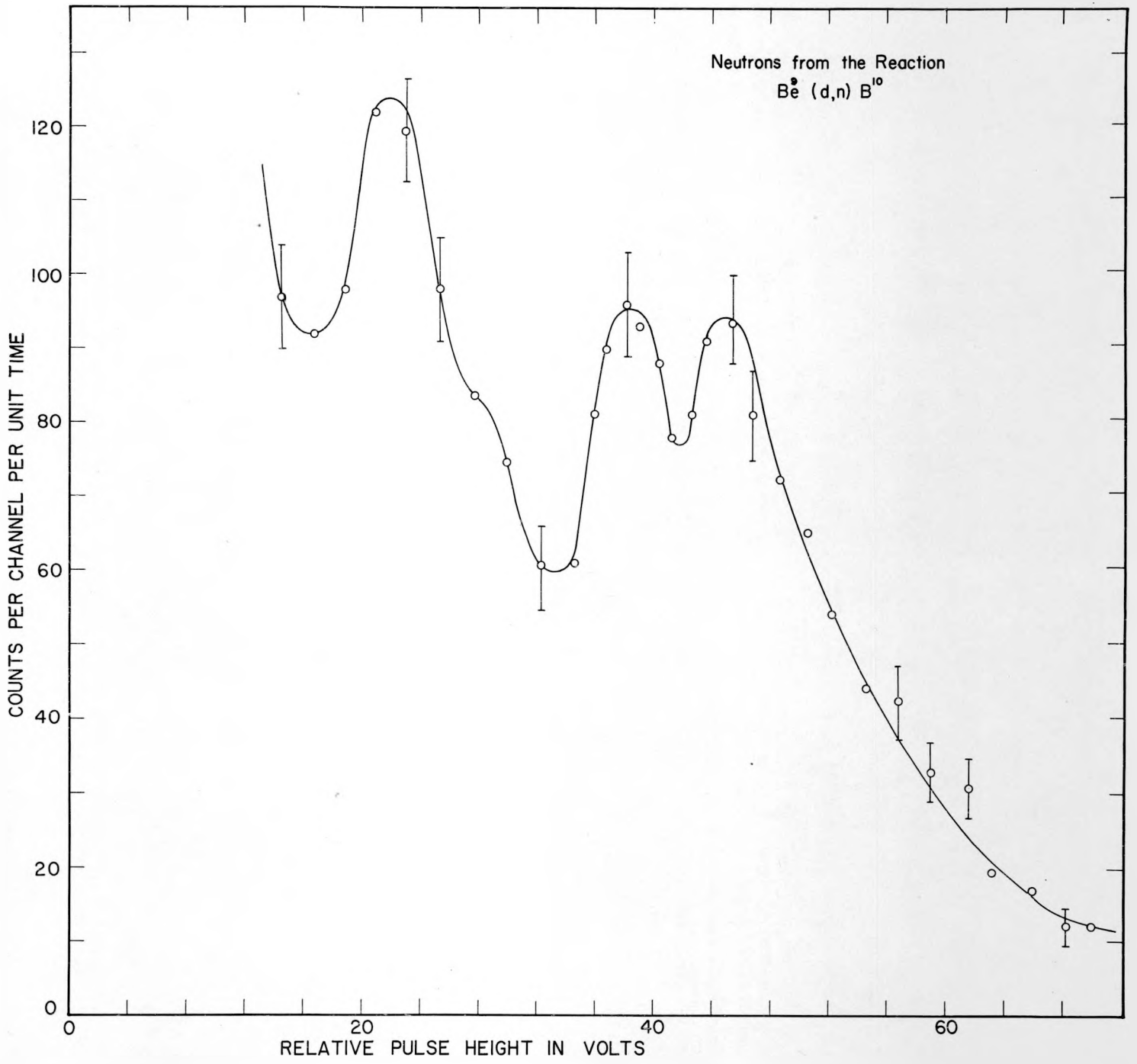
Neutrons from the Reaction
Be^{9} (d,n) B^{10}
COUNTS PER CHANNEL PER UNIT TIME
0
20
40
60
80
100
120
0
20
40
60
RELATIVE PULSE HEIGHT IN VOLTS

The design parameters of the neutron spectrometer may, in any case, be adjusted to obtain that compromise between resolution and efficiency which is deemed best for the experiment at hand. The values quoted here tend to favour resolution and sacrifice efficiency.

The resolution of the instrument (see Equation 2) is about 12 percent for 1 Mev gamma-rays, and we expect that it will be the same for monoenergetic neutrons from a thin target where the pulse heights are comparable to those of 1 Mev incident gammas.

This resolution is just sufficient for the study of neutrons produced in (d, n) reactions involving light nuclei, where the energy level spacings are quite large. One of the major problems remaining for this type of instrument is that of resolution.

In addition, an effort is being made to extend the region of application to neutron energies lower than the present limit of approximately 1 Mev.

We wish to thank Dr. Madansky for his many contributions to this project, and Dr. Swartz and Dr. Hanna for many helpful discussions and comments. Also we gratefully acknowledge the assistance of Mr. R. Slaven and Mr. R. Lee in the operation of the electrostatic generator.

ANGULAR DISTRIBUTION OF THE 0.72 Mev GAMMA RAY FROM THE REACTION $Be^9(d,n)B^{10*}(\ )B^{10}$

Introduction

The first angular distribution experiment performed with the neutron spectrometer was that of the 0.72 Mev gamma ray resulting from the bombardment of Beryllium with deuterons. This was selected because of the relative simplicity of the gamma ray spectrum of this reaction as recorded by the spectrometer. It would be very difficult to do this experiment with the usual NaI(Tl) scintillation counter, since the photoelectric peak at 0.72 Mev is superimposed on the Compton distributions of all the higher-energy gamma rays when this type of counter is used.

The energy level diagram is given in Figure 13, and a typical pulse-height distribution in Figure 14. The 0.41 Mev gamma ray produces pulses too small to be recorded; the 1.02 Mev line should have about one-half the intensity of the 0.72, but the efficiency of stilbene for gamma rays decreases rapidly with energy, so that the 1.02 Mev line appears still less intense.

Background Considerations

In order to measure the angular distribution, it is necessary to subtract the background and measure the intensity of the line for each angle of observation. The background is due to accidental coincidences; hence it should be a random sampling of the pulses from the primary counter, and should have the same form as the pulse-height distribution coming directly from the primary counter. This is shown as a dashed line in Figure 14. It was found that this distribution could be fitted quite accurately by the sum of two exponential functions, and such a form was used to estimate the background at each angle. The success of this method is indicated by the symmetrical shape of the subtracted curve, Figure 15.

Experimental Arrangement

For the actual experiment, a thick target of Beryllium was bombarded with 840 kev deuterons from the van de Graaff generator, at an average current of 0.25 microampere. Three series of runs were made, each series consisting of a 50 minute run at each of the following angles with respect to the deuteron beam: 0^o, 60^o, 90^o, 120^o, 160^o, 240^o, 270^o, and 300^o. The purpose of making runs on both sides of the beam was to detect any systematic errors related to the orientation of the spectrometer, but none were found. Before

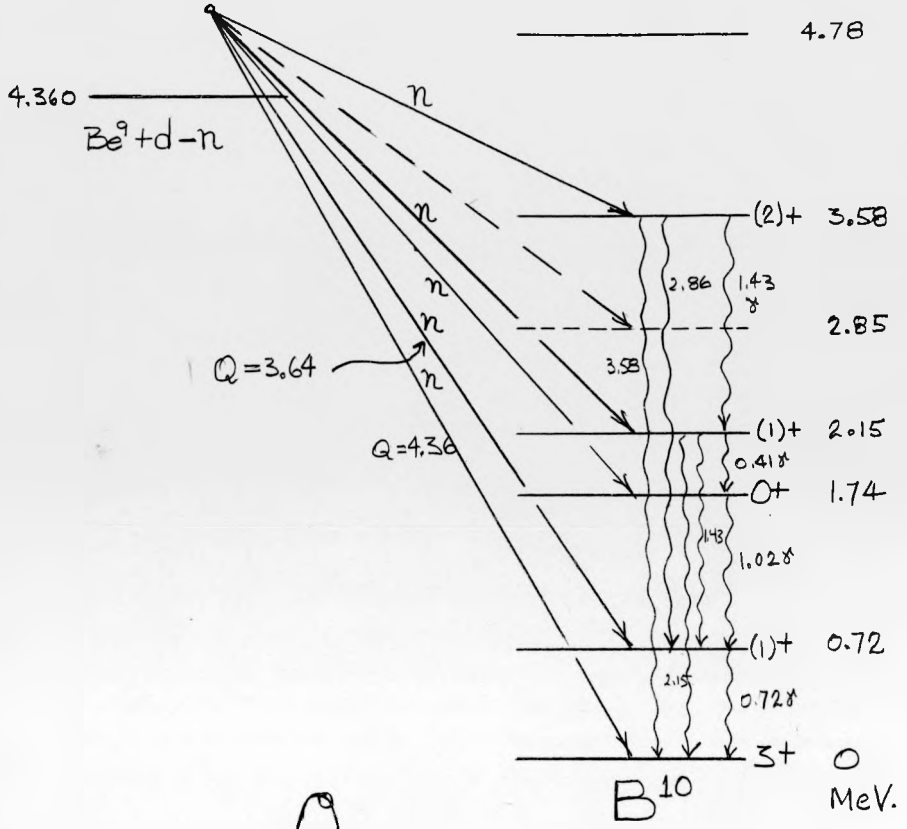

FIGURE 13. ENERGY LEVEL DIAGRAM FOR $Be^9(d,n)B^{10*}(\gamma)B^{10}$.

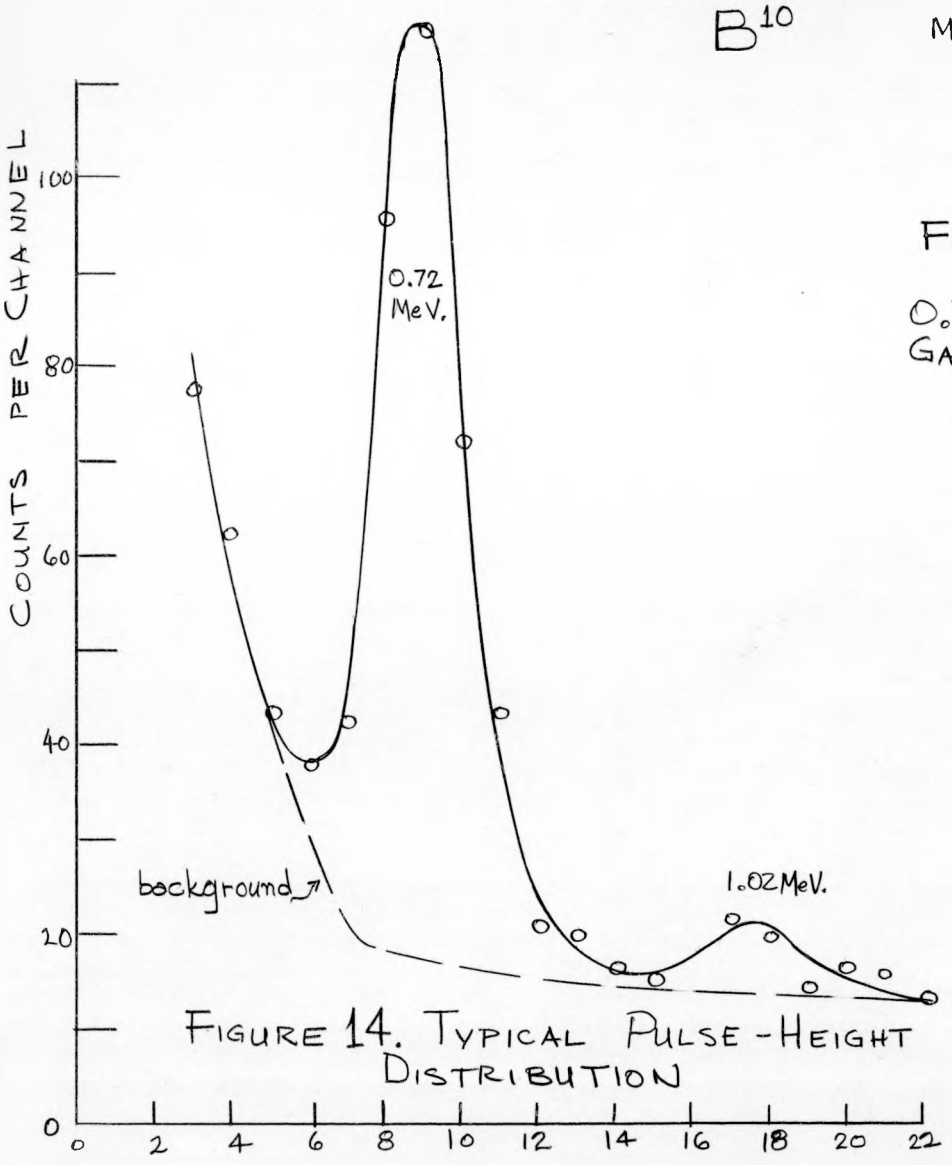

FIGURE 14. TYPICAL PULSE-HEIGHT DISTRIBUTION

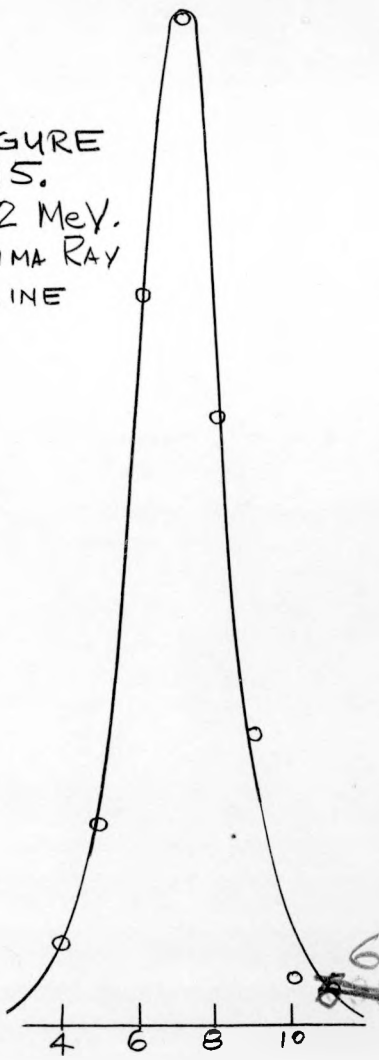

FIGURE 15. 0.72 MeV. GAMMA RAY LINE

and after each run, the 20-channel discriminator was calibrated, and the distance from the target to the primary counter was measured. The reaction was monitored by a single stilbene scintillation counter fixed directly above the target chamber, and by a current integrator measuring the total number of deuterons entering the target chamber. These two monitoring systems were found to be in agreement throughout the course of the experiment.

Treatment of Data

The raw data from each run were corrected for the height and width of each channel, then plotted and drawn as a smooth curve, as in Figure 14. Then the background was estimated as described above. The background intensity at the center of each channel was converted to a number of counts in that channel, and subtracted from the original number of counts therein. These differences were then added together to give the true counting rate for the gamma ray. On the average, about 400 true counts were obtained in each run. Then a correction was made for the changes in the distance from the target, among the different runs, and the result was normalized to the monitor counter counting rate. The resulting relative intensities are independent, to the first order of approximation, of any possible changes in the gain of the primary counter and of the linear amplifier, and of changes in the zero level of the gate circuit, as well as of drifts in the twenty-channel discriminator. This was verified by measuring, in the same manner, the "angular distribution" of the gamma rays from a radioactive source (Co^{60}), for which the same intensity was found in all directions, within statistical fluctuations.

Results

The relative intensity, $W(\theta)$, of the 0.72 Mev gamma ray at each angle in the laboratory system, averaged over the three series of runs, is as follows:

θ	$\cos\theta$	$W(\theta)$
0°	1.0	$1.01_5 \pm 0.3_5$
60° and 300°	0.5	$1.02_5 \pm 0.02$
90° and 270°	0	$1.01_5 \pm 0.02$
120° and 240°	-0.5	0.97 ± 0.02
160°	-0.95	0.99 ± 0.03

The center-of-mass transformation has been omitted; this has only of the order of a 1 percent effect and is in the direction such as to produce greater isotropy in the data. Thus the distribution is seen to be isotropic within about two percent.

The uncertainties quoted are only the statistical uncertainties in the number of counts at each point; the test with a radioactive source described above indicates that there are no systematic errors of comparable magnitude. A further confirmation of this, as well as of the isotropy of the radiation, is given by the internal consistency of the data: the statistical uncertainty attached to the intensity measurement in each individual run is about 5 percent; the root-mean-square deviation among the twenty-four runs is 4.6 percent. The internal consistency is thus established.

Interpretation

Referring to the Grotrian diagram, Figure 13, the 0.72 Mev gamma ray is emitted in a transition from the first excited state (assumed 1^+) to the ground state (3^+) of B^{10}, and hence should be electric quadrupole radiation ($l = 2$). The first excited state has substates with $m = 1$, 0 and -1. The $m = 0$ substate leads to an angular distribution $26 + 6 \cos^2\theta$, while $m = \pm 1$ gives $28 - 3 \cos^2\theta$. With equal populations of the substates, the angular distribution is of course isotropic.

The distribution is measured with respect to the deuteron beam, and the first excited state of B^{10} is formed in several ways; either by compound nucleus formation with the emission of a neutron ($Q = 3.64$ Mev) to the first excited state, or with the emission of a neutron of any of the lower Q values, with subsequent gamma ray emission to the same state. In addition, the same paths can be followed with the neutrons being emitted in stripping processes.

It appears that all these ways taken together make for an approximately random orientation of the B^{10*} nucleus. If the populations of the $m = 0$ and $m = \pm 1$ sublevels are in the ratio of 3 to 2, or vice versa, only a $\pm$ 3 percent correlation is expected.

We are very grateful to Dr. S. S. Hanna for suggesting this problem, and for the discussion given above.

A LINEAR GATE CIRCUIT FOR PULSE HEIGHT ANALYZERS

In many coincidence experiments it is necessary to measure the distribution in height of only those pulses from a scintillation counter which correspond to a certain coincidence or anticoincidence signal. When a multichannel analyzer is used to measure the pulse height distributions, this may be accomplished in two ways: the discriminator may be "keyed" or "gated" by the coincidence pulse so that it only operates immediately after the coincidence[1] or a gate circuit may be used which permits only the pulses corresponding to a coincidence to be amplified and sent to the discriminator.[2]

The first of these methods suffers from the disadvantage that the maximum single-counter rate (not the coincidence rate) is limited by the response time of the linear amplifier and analyzer. For example, an amplifier-discriminator system whose operating time is 100 microseconds (not unusually long) would be thoroughly jammed by a single-counter rate of 10^4 per second even though the coincidence rate were only a few counts per minute. The alternative method generally suffers from nonlinearity and instability of the gate circuit.

A balanced gate circuit having good linearity and stability has been developed in this laboratory for use with the fast neutron spectrometer. The block diagram of the spectrometer (Figure 6) illustrates the manner in which the gate is used. In this case, the height of the pulse from counter no. 1 is measured only when counter no. 1 is in coincidence with counter no. 2. The operation of the circuit can be clearly understood from the waveforms shown with the schematic diagram in Figure 16. The coincidence pulse operates a trigger circuit, the output of which cuts off the clamp tube V_1, thereby permitting the phase splitter V_2 to operate. The signal pulse, slightly delayed (about 0.15 microsec. with respect to the trigger pulse) is applied to one grid of V_2, resulting in signal pulses of opposite polarities at the two plates. The output of V_2 is fed to the difference amplifier V_3, so that the rectangular "pedestals" are subtracted, while the signal pulses are added. The output signal may be taken from either plate of V_3, giving a choice of polarity. The entire operation takes about 1 microsecond. Matched components are used, and the final balancing of the circuit is done with the 1000 potentiometer, after the tubes are well aged.

---

1. G. W. Hutchinson, Nucleonics 11, no. 2, p. 24
2. Guernsey, Mott, Nelson, and Roberts, Rev. Sci. Inst. 23, 476 (1952).

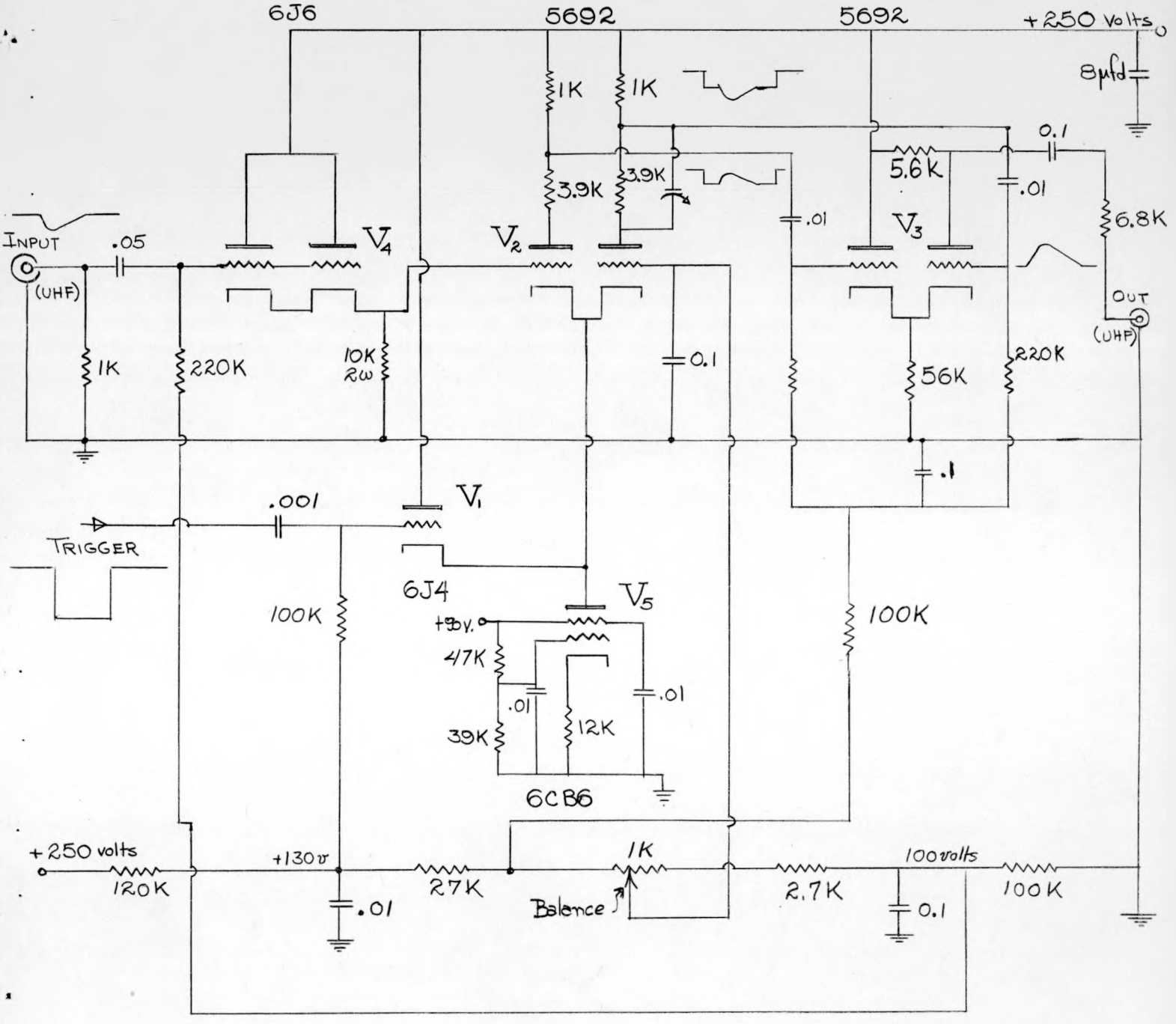

FIGURE 16: GATE CIRCUIT

The system is linear within 1 percent, over an input pulse-height range of about 50 : 1. After initial aging of the tubes the observed drift in the height of the residual pedestal is less than 1 percent of maximum output over a period of several hours, and perhaps 5 percent over several weeks. Unwanted pulses are completely rejected when negative input is used; for positive input, pulses up to about 10 volts are rejected.

Since no satisfactory way to apply inverse feedback around this circuit has been found, the gain depends directly on the characteristics of V_2 and V_3, and so can be expected to change slowly over long periods of time. With the tubes well ventilated, and with stabilized filament and plate power supplies, no change in gain has been noticed over periods of several days.

Many thanks are due to Mr. Ralph Segel and Dr. Berol Robinson for their suggestions and encouragement.